New Metal-Intercalated Layered Vanadyl Phosphates, $M_xVOPO_4 \cdot yH_2O$ (M = Ag, Cu, Zn)

P. Ayyappan and A. Ramanan*

Department of Chemistry, Indian Institute of Technology, New Delhi 110 016, India

C. C. Torardi*

Central Research and Development, DuPont Company, Experimental Station, Wilmington, Delaware 19880-0356

Received March 2, 1998

Three new, mixed-valent layered vanadyl phosphates, $Ag_{0.43}VOPO_4 \cdot 2H_2O$ (AgVPO), $Cu_{0.16}VOPO_4 \cdot 2.5H_2O$ (CuVPO), and $Zn_{0.11}VOPO_4 \cdot 2.5H_2O$ (ZnVPO), have been synthesized hydrothermally and their structures determined by single-crystal X-ray diffraction: AgVPO is triclinic, space group $P\bar{1}$, $a = 6.287(1)$, $b = 6.283(1)$, and $c = 13.240(1)$ Å, $\alpha = 80.98(1)$, $\beta = 86.58(1)$ and $\gamma = 90.00(1)°$, $Z = 4$; CuVPO is triclinic, space group $P\bar{1}$, $a = 6.260(2)$, $b = 6.249(3)$, and $c = 7.257(1)$ Å, $\alpha = 83.62(3)$, $\beta = 73.99(2)$, and $\gamma = 90.13(4)°$, $Z = 2$; ZnVPO is triclinic, space group $P1$, $a = 6.252(1)$, $b = 6.248(2)$, and $c = 7.339(3)$ Å, $\alpha = 83.24(4)$, $\beta = 73.93(2)$, and $\gamma = 90.00(2)°$, $Z = 2$. The structures are related to that of $VOPO_4 \cdot 2H_2O$. Metal powders have been found to be effective both as reductants and as countercations.

Introduction

Layered vanadyl phosphate, $VOPO_4 \cdot 2H_2O$, is a bilayer structure where the adjacent layers are held together by weak bonding interactions.[1] Each layer is composed of corner-sharing VO_6 octahedra and PO_4 tetrahedra. It crystallizes in the tetragonal space group $P4/nmm$ with $a = 6.202$ and $c = 7.410$ Å and $Z = 2$. An interesting feature of this bilayer structure is that ions/molecules can be incorporated into the interlamellar space through acid−base, ion-exchange, and redox reactions.[2−10] Some of these intercalated materials are well-known catalysts, and a few show unusual magnetic interactions.[11−15] In recent years, hydrothermal reactions have been found to be an effective route to prepare new intercalated materials as well as to grow suitable single crystals for detailed structural characterization.[3−10] However, the "black-box" nature of this method makes it challenging for chemists to develop varied synthetic pathways to control and rationalize the chemistry involved and, hence, the nature of the products.[16]

We have been investigating the formation of layered vanadyl phosphates under hydrothermal condition in the presence of several reducing agents, such as alkali borohydrides, metal powder, and tin chloride.[17] Use of metal powders (Ag, Cu, and Zn) has been found to be an effective way to reduce and directly precipitate single phasic $M_xVOPO_4 \cdot yH_2O$ crystals from aqueous vanadate solutions under hydrothermal conditions. Three new phases having the formulas $Ag_{0.43}VOPO_4 \cdot 2H_2O$ (AgVPO), $Cu_{0.16}VOPO_4 \cdot 2.5H_2O$ (CuVPO), and $Zn_{0.11}VOPO_4 \cdot 2.5H_2O$ (ZnVPO) have been synthesized hydrothermally for the first time. In this paper, we discuss our results on the synthesis and structural characterization of these hitherto unreported compounds.

Experimental Section

Synthesis. In all our preparations, reagent grade chemicals were used: V_2O_5 (CDH-India, 98.5%), Ag powder (Narrondass Manordass Refinery, Bombay, 98%), Cu granules (Perkin-Elmer), Zn dust (CDH−India, 98%), and H_3PO_4 (Qualigens-India, 88−93%). We reacted several mixtures containing varying molar proportions of M = Ag, Cu, or Zn with V (M/V = 0.25, 0.5, 0.75, and 1) by hydrothermal treatment with phosphoric acid. For the synthesis of AgVPO, we reacted 0.2587 g of V_2O_5 with 0.1533 g of Ag powder, 2 mL of H_3PO_4, and 30 mL of distilled water in the molar ratio V_2O_5:Ag:H_3PO_4:H_2O = 1:1:25:1176. CuVPO was prepared from a mixture of 0.5 g of V_2O_5, 0.1747 g of Cu powder, 2 mL of H_3PO_4, and 30 mL of water in the molar ratio V_2O_5:Cu:H_3PO_4:H_2O = 1:1:13:607. ZnVPO was prepared from a mixture of 0.3 g of V_2O_5, 0.1078 g of Zn dust, 2 mL of H_3PO_4, and 30 mL of water in the molar ratio V_2O_5:Zn:H_3PO_4:H_2O = 1:1:

(1) Ladwig, G. *Z. Anorg. Allg. Chem.* **1965**, *338*, 266.
(2) Jacobson, A. J.; Johnson, J. W. *Angew. Chem., Int. Ed. Engl.* **1983**, *22*, 412.
(3) Jacobson, A. J.; Johnson, J. W.; Brody, J. F.; Scanlon, J. C.; Lewandowski, J. T. *Inorg. Chem.* **1985**, *24*, 1782.
(4) Lii, K. H.; Tsai, H. J. *Inorg. Chem.* **1991**, *30*, 446.
(5) Wang, L.; Kang, H. Y.; Cheng, C. Y.; Lii, K. H. *Inorg. Chem.* **1991**, *30*, 3496.
(6) Lii, K. H.; Li, C. H.; Cheng, C. Y.; Wang, S. L. *J. Solid State Chem.* **1991**, *91*, 331.
(7) Lii, K. H.; Tsai, H. J. *J. Solid State Chem.* **1991**, *95*, 352.
(8) Lii, K. H.; Wen, N. S.; Su, C. C.; Chueh, B. R. *Inorg. Chem.* **1992**, *31*, 439.
(9) Kang, H. Y.; Lee, W. C.; Wang, S. L.; Lii, K. H. *Inorg. Chem.* **1992**, *31*, 4743.
(10) Zhang, Y.; Clearfield, A.; Haushalter, R. C. *J. Solid State Chem.* **1995**, *117*, 157.
(11) Antonia, M. R.; Barbour, R. L.; Blum, P. R. *Inorg. Chem.* **1987**, *26*, 1235.
(12) Papoutsakis, D.; Jackson, J. E.; Nocera, D. G. *Inorg. Chem.* **1996**, *35*, 800.
(13) Casan, N.; Amoros, P.; Ibanez, R.; Martinez, E.; Beltran-Porter, A.; Beltran-Porter, D. *J. Inclusion Phenom.* **1988**, *6*, 193.
(14) Beltran-Porter, D.; Amoros, P.; Ibanez, R.; Le Bail, A.; Ferey, G.; Villeneuve, G. *Solid State Ionics* **1989**, *32*, 57.
(15) Beltran-Porter, D.; Beltran-Porter, A.; Amoros, P.; Ibanez, R.; Martinez, E.; Le Bail, A.; Ferey, G.; Villeneuve, G. *Eur. J. Solid State Inorg. Chem.* **1991**, *28*, 131.
(16) Zubieta, J. *Comments Inorg. Chem.* **1994**, *16*, 153.
(17) Ayyappan, P.; Ramanan, A. (unpublished work).

S0020-1669(98)00228-6 CCC: $15.00
Published on Web 06/16/1998

Table 1. Chemical Analysis of AgVPO, CuVPO, and ZnVPO

compound	color	yield based on V (%)	average oxidation state of V: chemical analysis	average oxidation state of V: X-ray structure	total V: found	total V: calcd	total wt loss: found	total wt loss: calcd
$Ag_{0.43}VOPO_4{\cdot}2H_2O$ (AgVPO)	black	75	4.47	4.57	20.7	20.8	13.6	14.7
$Cu_{0.16}(H_2O)_{0.5}VOPO_4{\cdot}2H_2O$ (CuVPO)	green	50	4.63	4.68	23.8	23.4	21.6	20.6
$Zn_{0.11}(H_2O)_{0.5}VOPO_4{\cdot}2H_2O$ (ZnVPO)	green	65	4.73	4.78	25.5	23.8	19.7	21.0

21.6:1012. In all the cases, the mixture was transferred to a 45-mL Teflon-lined Parr acid digestion reactor, and the reaction vessel was heated at 180 °C for 10 h under autogenous pressure before cooling to room temperature at 10 °C/h. The dark-colored products were washed with water and then acetone and dried in air. Visual microscopic examination of the crystals prepared from various batches revealed the presence of uniform, dark green platy crystals (appeared green on grinding) which were quite fragile. The phases were characterized by powder and single-crystal X-ray diffraction, chemical analysis, thermal analysis, scanning electron microscopy (SEM), FTIR, and Raman spectroscopy. The amount of vanadium in the reduced state and the total vanadium content of the samples were determined by a potentiometric titration.[18] On the basis of chemical analyses and X-ray powder diffraction patterns, we inferred that essentially single phases with reasonable yields were obtained only when the initial molar ratio of metal to vanadium oxide was around 1.0. The samples appeared to be stable even after exposure to air for months. In Table 1, we show the color, the yield on the basis of vanadium, the average oxidation state of vanadium, the total vanadium content, and the total weight loss for AgVPO, CuVPO, and ZnVPO.

X-ray Powder Data. X-ray powder diffraction patterns (using a Philips PW1520) showed mainly 00*l* reflections with a layered periodicity of ~6.4 Å, indicating the formation of a phase similar to $VOPO_4{\cdot}2H_2O$. Room-temperature X-ray powder diffraction data for MVPO, M = Ag, Cu, and Zn, were also obtained using an APD3720 powder diffractometer with a θ-compensating slit, graphite monochromator, and Cu radiation in the range $2\theta = 2-90°$ for M = Ag and $2-60°$ for M = Cu and Zn. Silicon powder ($a = 5.4305$ Å) was used as an internal standard. Lattice parameters were obtained by least-squares treatment of the data, which consisted of K_α and $K_{\alpha1}$ peaks (i.e., $K_{\alpha2}$ peaks were omitted). The single-crystal X-ray parameters were used to initiate the refinements. Condensed tables of indexed X-ray powder diffraction data to a *d* spacing of 2.0 Å are given in Tables 2−4 for the Ag, Cu, and Zn compounds, respectively. Refined lattice parameters are included in the tables. Full tables of X-ray powder diffraction data are available as Supporting Information, Tables S1−S3. A very small amount of impurity was observed in each pattern. These lines were removed from the lattice parameter refinements. For AgVPO, only one very weak impurity line was seen, at $d = 3.20$ Å, which matches the strongest line of VO_2. CuVPO showed one very weak unidentified line at 4.64 Å. ZnVPO displayed five weak unidentified lines, the strongest at $d = 6.73$ Å having an intensity of ~5%, which could not be accounted for by a doubling or tripling of the cell constants.

Crystal Structures. Single-crystal X-ray diffraction data for AgVPO, CuVPO, and ZnVPO were collected using the experimental conditions given in Table 5. Automatic search, indexing, and centering routines were used to obtain the unit cells and orientation matrixes. Cell parameters for each compound were determined from 25 reflections with $13° < 2\theta < 30°$, $11° < 2\theta < 36°$, and $11° < 2\theta < 41°$ for M = Ag, Cu, and Zn, respectively. Although the *a*- and *b*-axes for all three triclinic unit cells are almost equal, and the γ angle for the Ag and Zn compounds is 90.0°; a unit cell of higher symmetry could not be found. For CuVPO, weak diffraction peaks indicated a tripling of the 7.2-Å *c*-axis. However, the quality of these crystals was not sufficient to determine the structure of the supercell, and only the subcell structure is reported here. No evidence of a supercell was found for isostructural ZnVPO, but a supercell may, indeed, exist. For each crystal, intensities of two standard reflections were periodically monitored and indicated no crystal decay. Data were corrected for Lorentz and polarization effects, and an analytical absorption correction was applied.[19] Full-matrix least-squares structural refinements were performed using a series

Table 2. Refined Lattice Parameters and Indexed X-ray Powder Diffraction Data for $Ag_{0.430(1)}VOPO_4{\cdot}2H_2O$ ($a = 6.296(1)$ Å, $b = 6.294(1)$ Å, $c = 13.265(2)$ Å, $\alpha = 80.95(1)°$, $\beta = 86.67(1)°$, $\gamma = 90.14(1)°$, $V = 518.2(1)$ Å^3)

I	*h*	*k*	*l*	d_{obs}	d_{calc}
57	0	0	2	6.542	6.539
6	1	0	0	6.294	6.284
1	1	0	1	5.813	5.799
1	1	0	−1	5.541	5.538
4	0	1	2	4.911	4.908
13	1	0	−2	4.405	4.403
	1	1	0		4.394
6	0	1	−2	4.194	4.187
5	−1	1	−1	4.120	4.120
4	1	1	2	3.936	3.936
8	0	1	3	3.866	3.867
3	1	0	3	3.690	3.685
3	1	1	−2	3.421	3.413
7	0	1	−3	3.330	3.331
100	0	0	4	3.270	3.269
13	0	2	0	3.105	3.108
	0	1	4		3.102
	2	0	1		3.097
18	0	2	2	2.995	2.996
	−1	1	−3		3.007
14	1	0	4	2.972	2.973
12	2	0	2	2.899	2.900
20	2	0	−2	2.768	2.769
	−2	1	1		2.765
	1	2	0		2.773
9	0	1	−4	2.722	2.722
	1	2	2		2.721
	−1	1	4		2.728
7	0	2	−2	2.650	2.650
3	0	1	5	2.558	2.559
	−1	1	−4		2.549
4	1	1	5	2.415	2.415
	1	2	−2		2.412
3	−2	1	3	2.380	2.386
4	−2	1	−3	2.348	2.346
3	1	2	4	2.314	2.314
3	0	1	−5	2.284	2.285
3	−2	2	1	2.219	2.217
	−2	2	0		2.222
	2	2	1		2.223
39	1	2	−3	2.180	2.181
	0	0	6		2.180
	0	2	5		2.177
	2	2	2		2.186
	−1	1	−5		2.187
2	3	0	0	2.096	2.095
	2	2	3		2.095
	1	0	6		2.098
	0	3	1		2.098
	0	2	−4		2.094
2	0	3	2	2.071	2.071
	2	0	5		2.071
	0	3	0		2.072
7	1	0	−6	2.022	2.023

plus 26 lines to $d = 1.170$ Å

(18) A known amount (~50 mg) of the sample was dissolved in a known excess of 0.01 M ceric ammonium sulfate and back-titrated against 0.01 M ferrous ammonium sulfate.

Table 3. Refined Lattice Parameters and Indexed X-ray Powder Diffraction Data for $Cu_{0.16(1)}VOPO_4 \cdot 2.5H_2O$ ($a = 6.272(3)$ Å, $b = 6.258(4)$ Å, $c = 7.242(3)$ Å, $\alpha = 83.14(6)°$, $\beta = 74.36(4)°$, $\gamma = 89.84(7)°$, $V = 271.6(3)$ Å^3)

I	h	k	l	d_{obs}	d_{calc}
100	0	0	1	6.916	6.920
1	0	1	0	6.212	6.210
1	1	0	0	6.059	6.037
2	1	0	1	5.317	5.320
4	0	1	1	4.946	4.934
4	−1	1	0	4.390	4.397
	0	1	−1		4.362
1	1	1	0	4.260	4.264
1	1	1	1	4.179	4.182
5	1	0	−1	4.025	4.039
2	−1	1	−1	3.905	3.911
50	0	0	2	3.463	3.460
5	1	0	2	3.422	3.430
1	1	1	−1	3.264	3.251
3	0	1	2	3.187	3.195
15	0	2	0	3.108	3.105
	1	1	2		3.145
12	2	0	1	3.091	3.091
9	2	0	0	3.020	3.018
8	0	2	1	2.970	2.973
2	0	1	−2	2.872	2.876
	−1	1	−2		2.878
4	1	0	−2	2.705	2.702
	0	2	−1		2.711
	1	2	0		2.727
	−2	1	−1		2.741
3	2	1	0	2.674	2.682
	2	0	2		2.660
1	−1	2	−1	2.598	2.606
	−1	1	2		2.584
	−1	2	1		2.580
2	2	0	−1	2.524	2.527
	2	1	2		2.507
1	0	2	2	2.457	2.467
	1	2	2		2.432
3	−2	1	1	2.398	2.401
3	1	0	3	2.377	2.381
	1	1	−2		2.384
	−2	1	−2		2.387
2	1	2	−1	2.359	2.358
7	1	1	3	2.314	2.314
	0	0	3		2.307
4	0	1	3	2.263	2.255
	2	1	−1		2.285
2	2	2	1	2.214	2.217
	−2	2	0		2.199
2	0	2	−2	2.176	2.181
	−2	2	−1		2.165
	−1	2	−2		2.191
	−1	2	2		2.159
2	2	2	0	2.132	2.132
	2	0	3		2.133
	−1	1	−3		2.142
4	2	2	2	2.093	2.091
4	3	0	1	2.090	2.090
	0	1	−3		2.080
	2	1	3		2.077
	0	3	0		2.070
2	2	0	−2	2.016	2.019
	3	0	0		2.012
	1	2	3		2.004
	−2	2	1		2.031

plus 12 lines to $d = 1.558$ Å

Table 4. Refined Lattice Parameters and Indexed X-ray Powder Diffraction Data for $Zn_{0.11(1)}VOPO_4 \cdot 2.5H_2O$ ($a = 6.243(5)$ Å, $b = 6.249(4)$ Å, $c = 7.350(4)$ Å, $\alpha = 83.34(6)°$, $\beta = 74.49(8)°$, $\gamma = 90.51(9)°$, $V = 274.2(4)$ Å^3)

I	h	k	l	d_{obs}	d_{calc}
100	0	0	1	7.052	7.029
1	1	0	0	6.044	6.011
	0	1	0		6.201
1	1	0	1	5.388	5.336
1	0	1	1	4.977	4.963
2	−1	1	0	4.402	4.409
	0	1	−1		4.390
1	1	1	0	4.210	4.229
	1	1	1		4.162
1	1	0	−1	4.049	4.058
34	0	0	2	3.512	3.514
	1	0	2		3.470
	−1	1	1		3.561
1	0	1	2	3.231	3.233
	1	1	−1		3.251
4	0	2	0	3.099	3.101
	2	0	1		3.081
	1	1	2		3.162
3	2	0	0	3.008	3.005
3	0	2	1	2.978	2.975
1	0	1	−2	2.906	2.908
	−1	1	−2		2.910
2	0	2	−1	2.718	2.716
	1	2	0		2.710
	1	0	−2		2.729
	−2	1	−1		2.747
	1	2	1		2.749
	−2	1	0		2.750
1	2	0	2	2.685	2.668
	2	1	0		2.661
1	−1	2	1	2.581	2.591
	−1	1	2		2.611
	−1	2	−1		2.618
1	2	0	−1	2.521	2.527
	2	1	2		2.502
1	0	2	2	2.483	2.481
1	1	2	2	2.421	2.433
1	1	0	3	2.418	2.415
	−2	1	1		2.408
	−2	1	−2		2.402
	1	1	−2		2.399
5	1	1	3	2.338	2.339
	0	0	3		2.343
	1	2	−1		2.354
2	2	1	−1	2.282	2.278
	0	1	3		2.287
1	−1	2	−2	2.211	2.208
	−2	2	0		2.204
1	0	2	−2	2.195	2.195
	2	2	1		2.198
1	−1	1	−3	2.168	2.171
	−2	2	−1		2.173
	−1	2	2		2.176
	2	0	3		2.151
1	0	1	−3	2.105	2.108
	2	2	0		2.114
	2	1	3		2.087
1	0	3	1	2.059	2.053
	0	3	0		2.067
	−2	2	1		2.040
	3	0	1		2.081
	2	2	2		2.081
1	1	2	3	2.020	2.016
	2	0	−2		2.029
2	3	0	0	2.000	2.004
	1	0	−3		2.007
	0	2	3		1.991

plus 18 lines to $d = 1.552$ Å

of programs developed by J. C. Calabrese,[20] and thermal ellipsoid plots were drawn using ORTEP-III.[21]

Starting atomic positions for the V and P atoms were obtained by the heavy-atom method, and O atoms were located from difference Fourier analyses. It was not possible to determine the H atom positions for the M = Cu and Zn phases, and only three out of eight hydrogen

(19) De Meulenaer, J.; Tompa, H. *Acta Crystallogr.* **1965**, *19*, 1014.

Table 5. Crystallographic Data for $Ag_{0.430(1)}VOPO_4{\cdot}2H_2O$, $Cu_{0.16(1)}VOPO_4{\cdot}2.5H_2O$, and $Zn_{0.11(1)}VOPO_4{\cdot}2.5H_2O$

chemical formula	$Ag_{0.430(1)}VOPO_4{\cdot}2H_2O$	$Cu_{0.16(1)}VOPO_4{\cdot}2.5H_2O$	$Zn_{0.11(1)}VOPO_4{\cdot}2.5H_2O$
formula weight	244.32	217.75	214.14
space group	$P\bar{1}$	$P\bar{1}$	$P\bar{1}$
a (Å)	6.287(1)	6.260(2)	6.252(1)
b (Å)	6.283(1)	6.249(3)	6.248(2)
c (Å)	13.240(1)	7.257(1)	7.339(3)
α (deg)	80.98(1)	83.62(3)	83.24(4)
β (deg)	86.58(1)	73.99(2)	73.93(2)
γ (deg)	90.00(1)	90.13(4)	90.00(2)
V (Å^3)	515.59	271.02	273.40
temp (°C)	20	20	20
Z	4	2	2
ρ_{calc} (g cm^{-3})	3.147	2.668	2.601
λ (Å)	0.710 69	0.710 69	0.710 69
linear abs coeff (cm^{-1})	37.14	26.98	25.12
R (F_o), R_w[a] (F_o) (%)	2.69, 3.00	7.86, 5.38	5.13, 4.42

[a] $R_w = [\sum w(|F_o| - |F_c|)^2/\sum w|F_o|^2]^{1/2}$, with w proportional to $1/[\sigma^2(I) + (0.02I)^2]$.

Table 6. Fractional Coordinates (×10 000) and Isotropic Thermal Parameters[a] (×1000) for $Ag_{0.430(1)}VOPO_4{\cdot}2H_2O$

atom	x	y	z	U_{iso}
Ag(1)[b]	5756.8(7)	9743.0(6)	2518.3(4)	41.8(2)
V(1)	7613.2(8)	12634.6(7)	4532.7(4)	6.3(2)
V(2)	2428.3(8)	12418.5(7)	469.0(4)	6.3(2)
P(1)	7483.8(11)	7487.3(11)	5018.3(6)	6.3(3)
P(2)	7499.3(11)	12478.1(11)	19.8(6)	6.3(3)
O(1)	7501(4)	12231(4)	5742(2)	15(1)
O(2)	7773(3)	5793(3)	4304(2)	12(1)
O(3)	7467(3)	9659(3)	4303(2)	11(1)
O(4)	9287(3)	7388(3)	5757(2)	11(1)
O(5)	5427(3)	7108(3)	5705(2)	13(1)
O(6)	5454(3)	12236(3)	725(2)	11(1)
O(7)	9328(3)	12421(3)	738(2)	12(1)
O(8)	2544(4)	12920(4)	−737(2)	16(1)
O(9)	7528(3)	14593(3)	−746(2)	12(1)
O(10)	7684(3)	10705(3)	−647(2)	12(1)
O(11)	2185(4)	11416(4)	2267(2)	17(1)
O(12)	7636(4)	13235(4)	2740(2)	19(1)
O(13)	4458(4)	6163(4)	2490(2)	22(1)
O(14)	9489(5)	8076(5)	2484(2)	32(1)
H(1)	9071(82)	7566(80)	2017(40)	50(0)
H(2)	6803(82)	14121(79)	2581(39)	50(0)
H(3)	1735(88)	11720(89)	2685(41)	50(0)

[a] Thermal parameters for H atoms fixed. [b] Refined site multiplier = 0.859(2).

atoms were located in the M = Ag compound. All atom occupancies were checked, and only the Ag, Cu, and Zn sites were found to be partially occupied. Atomic positional and isotropic thermal parameters for the M = Ag, Cu, and Zn structures are given in Tables 6−8. Tables in the Supporting Information include complete crystallographic data (Table S4), anisotropic thermal parameters (Tables S5−S7), interatomic distances (Tables S8−S10), and bond angles (Tables S11−S13).

Thermal Analysis. Thermogravimetric (TG) analyses were carried out using DuPont TG system 2100 on well-ground samples in flowing nitrogen atmosphere (30 mL/min) with a heating rate of 5 °C/min.

FTIR and Raman Spectra. FTIR spectra were recorded on KBr pellets (Perkin-Elmer 16PC FTIR), while Raman spectra were recorded on a backscattering geometry (Renishaw) using a light source of 12 787.72 cm^{-1}.

Table 7. Fractional Coordinates (×10 000) and Isotropic Thermal Parameters (×1000) for $Cu_{0.16(1)}VOPO_4{\cdot}2.5H_2O$

atom	x	y	z	U_{iso}
Cu(1)[a]	1292(8)	7262(8)	−126(8)	14(1)
Cu(2)[b]	3056(11)	11143(11)	−80(11)	14(3)
V(1)	2769(1)	7660(1)	4134(1)	12.7(3)
P(1)	2509(2)	12515(2)	4983(2)	15.2(5)
O(1)	2899(5)	10755(4)	3640(5)	23(1)
O(2)	4040(5)	12311(4)	6291(4)	19(1)
O(3)	2931(5)	14657(4)	3690(5)	20(1)
O(4)	163(5)	12335(4)	6298(4)	19(1)
O(5)	2019(5)	7398(5)	6430(5)	24(1)
O(6)	6167(6)	11917(5)	−815(5)	34(1)
O(7)	2147(7)	4272(7)	−46(6)	55(1)
O(8)	0(0)	10000(0)	0(0)	62(3)

[a] Refined site multiplier = 0.094(2). [b] Refined site multiplier = 0.069(2).

Table 8. Fractional Coordinates (×10 000) and Isotropic Thermal Parameters (×1000) for $Zn_{0.11(1)}VOPO_4{\cdot}2.5H_2O$

atom	x	y	z	U_{iso}
Zn(1)[a]	6779(20)	8714(19)	−109(20)	35(6)
V(1)	2767(3)	7676(3)	4150(3)	14(1)
P(1)	2512(5)	12515(5)	5003(4)	18(1)
O(1)	2858(10)	10773(10)	3646(9)	20(3)
O(2)	4044(11)	12244(10)	6299(10)	19(3)
O(3)	2996(11)	14683(10)	3714(10)	22(3)
O(4)	122(10)	12365(10)	6298(10)	22(3)
O(5)	2013(14)	7416(12)	6406(11)	23(3)
O(6)	3817(14)	8069(12)	852(10)	42(4)
O(7)	7793(14)	5553(14)	77(11)	52(4)
O(8)	0(0)	0(0)	0(0)	52(6)

[a] Refined site multiplier = 0.109(5).

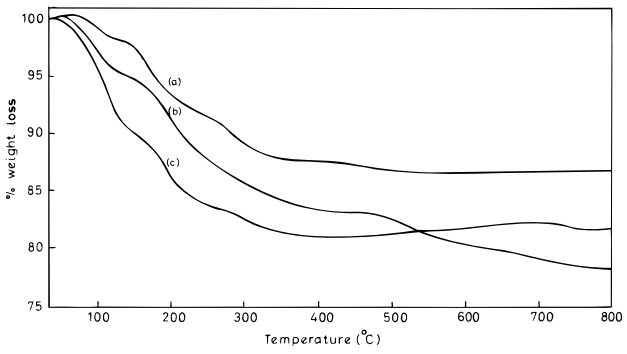

Figure 1. TGA curves of (a) $Ag_{0.43}VOPO_4{\cdot}2H_2O$, (b) $Cu_{0.16}VOPO_4{\cdot}2.5H_2O$, and (c) $Zn_{0.11}VOPO_4{\cdot}2.5H_2O$.

Results and Discussion

The thermograms of these compounds (Figure 1) indicate that, in all cases, loss of water takes place in two or three steps (in this region, DTA showed a broad endothermic peak). All the materials decomposed above 600 °C. The difference in thermal behavior is mainly due to varying interactions between the intercalated cations and the coordinated water molecules. The observed total weight losses for the samples between room temperature and 500 °C agree with those calculated from the formulas (refer to Table 1).

FTIR and Raman spectroscopy is frequently used to establish local structural similarities among vanadyl phosphates. Laser Raman spectra of AgVPO, CuVPO, and ZnVPO are shown in Figure 2. FTIR spectra of all the three samples are similar and showed a strong resemblance to the FTIR spectra of other metal-

(20) All X-ray crystallographic calculations were performed on a Digital Equipment Corp. VAX 6630 computer using a system of programs developed by J. C. Calabrese.

(21) Burnett, M. N.; Johnson, C. K. *ORTEP-III: Oak Ridge Thermal Ellipsoid Plot Program for Crystal Structure Illustrations;* Oak Ridge National Laboratory Report ORNL-6895; Oak Ridge National Laboratory: Oak Ridge, TN, 1996.

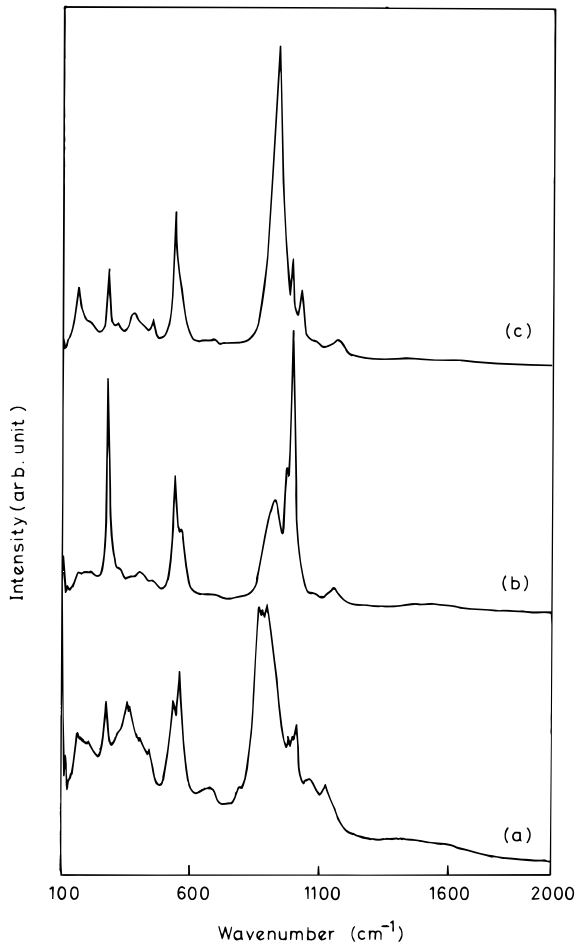

Figure 2. Raman spectra of (a) $Ag_{0.43}VOPO_4{\cdot}2H_2O$, (b) $Cu_{0.16}VOPO_4{\cdot}2.5H_2O$, and (c) $Zn_{0.11}VOPO_4{\cdot}2.5H_2O$.

intercalated vanadyl phosphates.[2,3,22] The absorptions around 3500−3400, 1640 cm^{-1} correspond to stretching and bending modes of water. The strong bands around 1090 and 1055 cm^{-1} are assigned to ν_3 of PO_4 groups.[23] The bands occurring around 990 cm^{-1} are due to V═O stretch. The broad, weak band around 680 cm^{-1} is due to the V−O−P lattice.[6,7] The prominent absorptions of Raman spectra[24] could be assigned[25] to P−O stretch in the 1200−1000 cm^{-1} range, V═O stretch at 1000−990 cm^{-1}, and P−O stretch at 985−975 cm^{-1}, as well as coupling with V−O and P−O bending modes and skeletal vibrations in the range 600−150 cm^{-1}. SEM micrographs of AgVPO, CuVPO, and ZnVPO indicate the formation of well-defined crystals with platy habit (Figure 3).

Descriptions of the Structures. The structures of $M_xVOPO_4{\cdot}yH_2O$ (M = Ag, Cu, Zn) have a different layer stacking sequence from that found in the parent $VOPO_4{\cdot}2H_2O$. In $VOPO_4{\cdot}2H_2O$, the VPO layers stack *directly* on top of each other so that each V═O group is oriented toward the water molecule, which is weakly coordinated trans to the V═O group of an adjacent layer. In the Cu and Zn compounds, adjacent

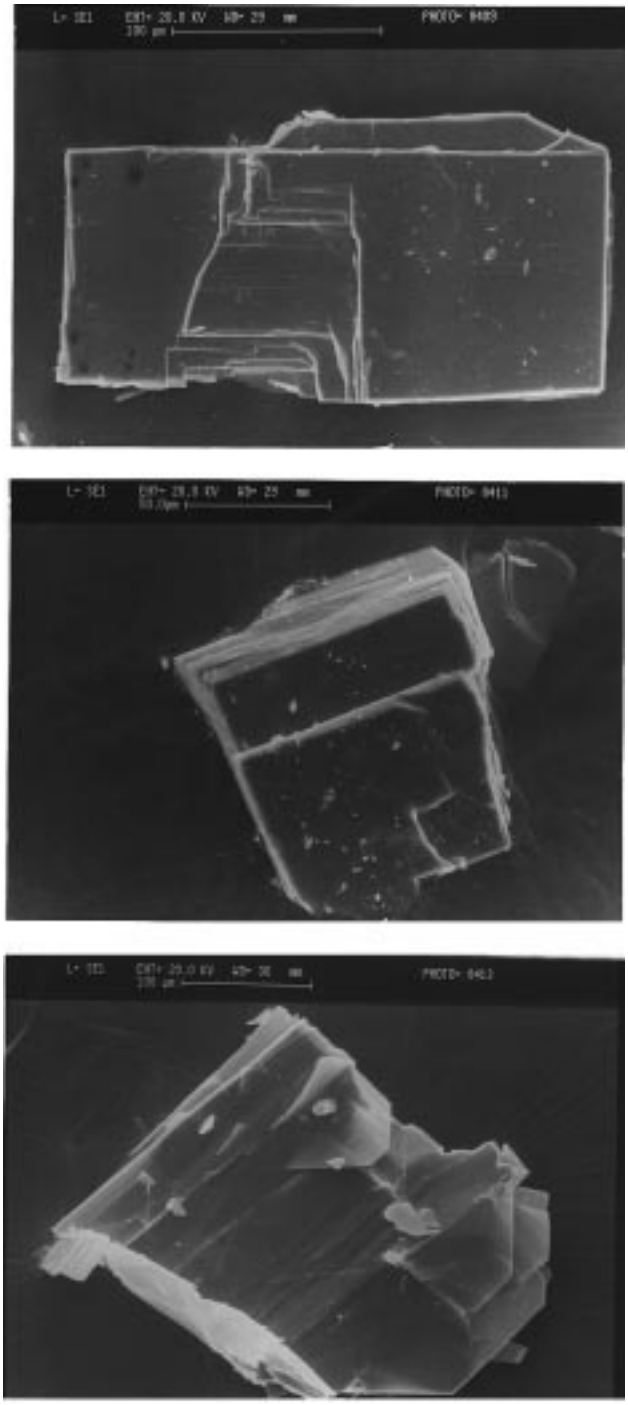

Figure 3. Scanning electron micrographs of (top) $Ag_{0.43}VOPO_4{\cdot}2H_2O$, (middle) $Cu_{0.16}VOPO_4{\cdot}2.5H_2O$, and (bottom) $Zn_{0.11}VOPO_4{\cdot}2.5H_2O$.

layers are offset from one another so that all atoms of the same kind (e.g., all V or all P) form strings parallel with the triclinic *c*-axis (Figure 4). However, the VPO layers in the M = Ag compound are offset so that alternating V and P atoms lie in strings parallel with the triclinic *c*-axis (Figure 5). This results in the doubling of the *c*-axis in AgVPO relative to those in CuVPO (subcell) and ZnVPO.

In AgVPO, incorporation of silver cations into the interlayer space not only leads to partial reduction of V^{5+} to V^{4+} but also alters the way the water molecules are packed between the layers. Interlayer separation is considerably smaller, as expected due to electrostatic interaction between silver and the negatively charged vanadyl phosphate layer. Although the atomic coordinates of AgVPO are very close to those of $Na_{0.5}$-

(22) Chauvel, A.; de Roy, M. E.; Besse, J. P.; Benarbia, A.; Legrouri, A.; Barroug, A. *Mater. Chem. Phys.* **1995**, *40*, 207.
(23) Wrobleski, J. T. *Inorg. Chem.* **1988**, *27*, 946.
(24) Raman spectra of AgVPO showed features around 1130(vw), 1020(w), 990(w), 930(s, broad), 540(m), 450(w), 370(w), 280(w), and 160(w) cm^{-1}; CuVPO showed peaks around 1156(vw), 995(vs), 970(vs), 930(m, broad), 565(w), 540(s), 410(w), 280(s), and 165(w) cm^{-1}; ZnVO showed peaks around 1170(vw), 1020(w), 990(m), 940(vs), 565(m), 535(w), 450(w), 370(w), 280(w), and 165(w) cm^{-1}.
(25) Sundaresan, G. *Chem. Mater.* **1995**, *7*, 995.

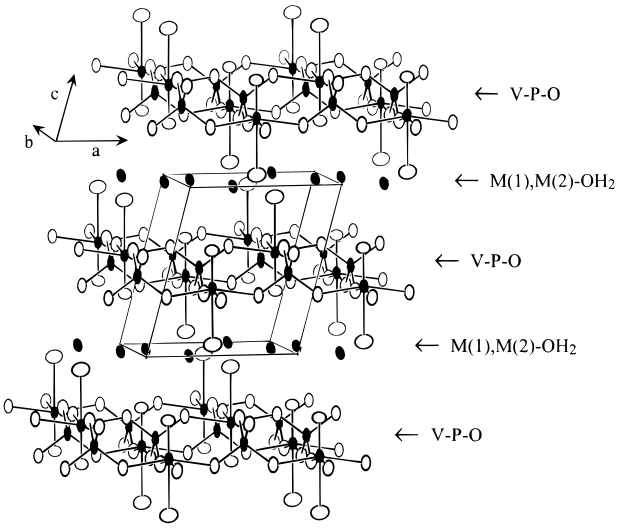

Figure 4. ORTEP plot (50% probability thermal ellipsoids) of $M_xVOPO_4 \cdot 2.5H_2O$ (M = Cu or Zn), showing the triclinic unit cell, stacking of VPO layers, and the interlayer, partially occupied M sites. Vanadium is octahedrally coordinated, and phosphorus is tetrahedrally coordinated (M, V, and P atoms are shaded).

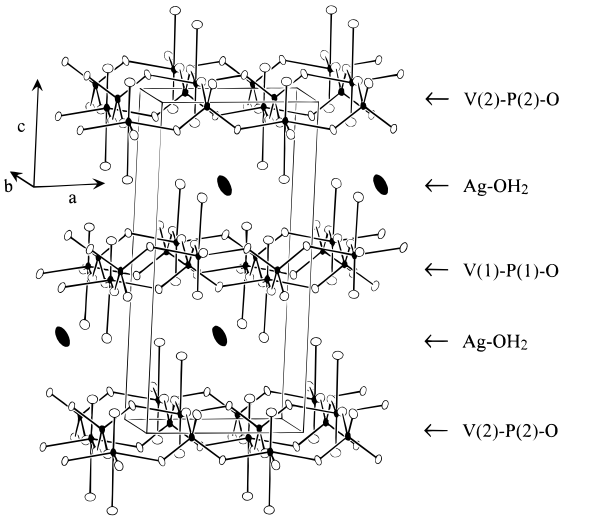

Figure 5. ORTEP plot (50% probability thermal ellipsoids) of $Ag_{0.43}VOPO_4 \cdot 2H_2O$ showing the triclinic unit cell, stacking of VPO layers, and the interlayer, partially occupied Ag sites. Vanadium is octahedrally coordinated, and phosphorus is tetrahedrally coordinated (Ag, V, and P atoms are shaded).

$VOPO_4 \cdot 2H_2O$,[5] TG data suggest that both lattice and coordinated water molecules are more strongly bonded in the former case. In AgVPO, the Ag ion occurs in a distorted octahedral coordination (Figure 6); four oxygens, belonging to water molecules, form the shorter bonds to Ag (2.40−2.57 Å), while the other two oxygens, belonging to the VPO layer framework, form longer bonds (2.65 Å). Of the four water molecules associated with Ag, two are bonded to vanadium: one V from each adjacent layer. The V atoms in AgVPO have a distorted coordination geometry, with a short V−O bond length (∼1.58 Å), a long V−O bond (∼2.33 Å), and four equatorial bonds (∼1.96 Å). The oxygen atoms trans to the short V−O bonds belong to water molecules. Bond order sums[26] for vanadium are in accordance with an average oxidation state of ∼+4.6. In all probability, the V^{5+} and V^{4+} are disordered within the layers.

(26) Brown, I. D.; Altermatt, D. *Acta Crystallogr.* **1985**, *B41*, 244.

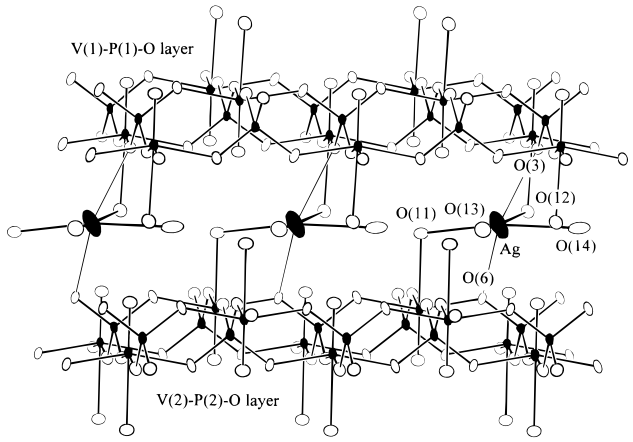

Figure 6. ORTEP plot (50% probability thermal ellipsoids) of $Ag_{0.43}VOPO_4 \cdot 2H_2O$, showing two VPO layers and the interlayer $Ag(H_2O)_4^+$ units. Vanadium is octahedrally coordinated, and phosphorus is tetrahedrally coordinated (Ag, V, and P atoms are shaded).

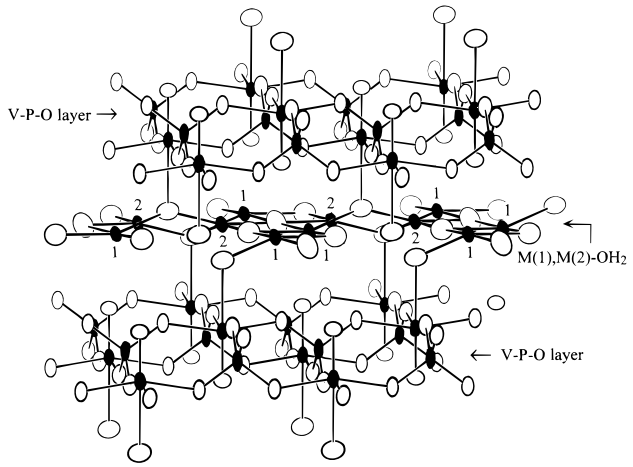

Figure 7. ORTEP plot (50% probability thermal ellipsoids) of $M_xVOPO_4 \cdot 2.5H_2O$ (M = Cu or Zn), showing two VPO layers and the interlayer $M(H_2O)_4^{2+}$ units. The CuVPO subcell structure has copper in partially occupied sites 1 and 2, while ZnVPO has zinc only in partially occupied site 2. Vanadium is octahedrally coordinated, and phosphorus is tetrahedrally coordinated (M, V, and P atoms are shaded).

The structures of ZnVPO and subcell structure of CuVPO are comparable to that of $K_{0.5}VOPO_4 \cdot 1.5H_2O$,[5] except that the transition metal atoms are coordinated in a different manner, and they also take up more water molecules within the layer (Figure 7). In $K_{0.5}VOPO_4 \cdot 1.5H_2O$, K is bonded to six oxygen atoms (four framework oxygens and two water molecules), with all six K−O bonds of comparable length. In ZnVPO, Zn takes up a distorted 4 + 2 octahedral coordination, with four short bonds (∼2.0 Å) to water molecules arranged in equatorial positions around Zn and two long bonds (∼2.6 Å) to framework oxygen atoms situated in apical positions around Zn. Of the four water molecules coordinated to Zn, two are bonded to vanadium and two are isolated. In the CuVPO subcell structure, divalent Cu partially occupies two crystallographically different sites, each site having essentially the same bonding environment as Zn in ZnVPO. The tripled *c*-axis supercell, discussed above, may be due to an ordering of the Cu atoms. It should be noted here that, in a recent report, Zhang et al.[10] have obtained two entirely new compounds, $Cu_{0.5}[VOPO_4] \cdot 2H_2O$, and $Cu_{0.5}(OH)_{0.5}[VOPO_4] \cdot 2H_2O$ using hydrothermal reactions. The former has a layered structure consisting of layers of $VOPO_4$ with Cu^{2+} ions between the layers, while the latter has similar $VOPO_4$

layers that are linked together by the unusual μ^3-OH-bridged Cu dimers of the composition $Cu_2(OH)_2(H_2O)_4$.

We also carried out bond valence analyses[26] to obtain a better understanding of the structure with respect to the cationic coordination, the location of water molecules, and the presence of hydroxo groups. The results of these analyses agree quite well with the overall compositions and average oxidation states of vanadium estimated from the single-crystal X-ray data (see Table 1). The agreement clearly indicates that there are no HPO_4 entities, as commonly found in other related structures.[27,28]

Formation of Layered Vanadyl Phosphates. Hydrothermal synthesis of metal-intercalated vanadyl phosphates involves several variables. Redox chemistry and the pH of the starting solution appear to play major roles in the formation of the product. So far, most research groups have employed V metal, VO_2, or V_2O_3 to prepare reduced vanadyl phosphates, and the metal ions are invariably taken as oxides or hydroxides. In our studies, we employed metals (Mg,[29] Fe, Co, Ni, Cu, Zn, Cd, Ag) having lower reduction potential than that corresponding to the $\epsilon^o(VO_2^+/VO^{2+}) = 0.9994$ V pair found in aqueous vanadate solution. Our intention was to use the metals both as reducing agents and as countercations to form the intercalated compounds. While essentially single-phasic crystals could be obtained with Cu, Zn, and Ag, only polycrystalline or multiphasic powders were synthesized with Mg, Ni, Fe, Co, and Cd.[17] Also, there was no success in obtaining single crystals with the latter ones. We used varying metal ratios in our attempts to control the oxidation state of vanadium. Our results indicated that, invariably, we got only mixed-valent materials, as indicated from chemical analyses. Recently, Roca et al.[30,31] have observed that lower pH values in the range 1.0−4.5 favored the formation of layered phases related to $VOPO_4 \cdot 2H_2O$. Livage et al.[32] concluded, on the basis of partial-charge model calculations, that, at very low pH values, the dominant species present in the aqueous solution undergoes successive hydrolysis and condensation to form the 2-D anion $[VO(H_2O)PO_4]_n^{n-}$, precursor of all lamellar solids showing the typical framework derived from that of parent $VOPO_4 \cdot 2H_2O$. We believe this hydrolysis−condensation sequence is operative even in the presence of guest ions Ag, Cu, or Zn employed in this study.[33] The oxygen redox couple in aqueous solution, $\epsilon^o(O_2/H_2O) = 1.229$ V, probably oxidizes part of V(IV) into V(V), thereby limiting the amount of metal cations which is ultimately intercalated between the layers. Unlike Cu and Ag ($\epsilon^o(Cu^{2+}/Cu = +0.34$ V); $\epsilon^o(Ag^+/Ag = +0.80$ V)), Zn ($\epsilon^o(Zn^{2+}/Zn = -0.76$ V)) is known to generate nascent hydrogen which, in turn, can reduce vanadate ions. The small differences between the average oxidation state of vanadium between chemical analysis and the structure may be due to the presence of unreacted metallic impurities. It should be noted here that, on the basis of valence matching principle, Roca et al.[31] concluded that higher Lewis acid strength cations such as Mg^{2+} and Zn^{2+} could not be incorporated between the layers. Contrary to their calculations, we have obtained Zn- and Mg-intercalated vanadyl phosphates by starting with metal powders rather than metal salts. It appears that, in addition to pH, the nature of the starting materials (like reducing agents) is important in determining the final products. pH dictates the thermodynamic stability of the phases, while the nature of the starting materials is probably important in controlling the kinetics of the initial reactions. The use of metal powders and alkali borohydrides[34] is responsible for the better reactivity in the initial stages.

Acknowledgment. A.R. thanks the Board of Research and Nuclear Sciences, Government of India, for financial support and a fellowship to P.A. A.R. thanks Dr. Allan Pring, South Australia Museum, Adelaide, for extending X-ray power diffraction assistance for preliminary characterization. We thank W. J. Marshall for collecting the single-crystal X-ray diffraction data, C. M. Foris for powder X-ray diffraction data, and Dr. T. P. Anathanarayan (Ranbaxy, Gurgaon) and Mr. Xian Ben Wang (Department of Physics, National University of Singapore) for help with FTIR and Raman measurements, respectively. A.R. thanks the Department of Materials Science, National University of Singapore, for TG measurements.

Supporting Information Available: Listings of full X-ray powder diffraction data, complete crystallographic parameters, anisotropic thermal parameters, interatomic distances, and bond angles (18 pages). Ordering information is given on any current masthead page.

IC980228B

(27) Vaughey, J. T.; Harrison, W. T. A.; Jacobson, A. J. *J. Solid State Chem.* **1994**, *110*, 305.
(28) Haushalter, R. C.; Wang, S.; Thompson, M. E.; Zubieta, J.; O'Connor, C. T, *J. Solid State Chem.* **1994**, *109*, 259.
(29) Preliminary XRD suggest that MgVPO is isostructural to ZnVPO, with interlayer spacing ~7.10 Å.
(30) Roca, M.; Marcos, D.; Amoros, P.; Beltran-Porter, A.; Edwards, A.; Beltran-Porter, D. *Inorg. Chem.* **1996**, *35*, 5613.
(31) Roca, M.; Marcos, M. D.; Amoros, P.; Alamo, A.; Beltran-Porter, B.; Beltran-Porter, D. *Inorg. Chem.* **1997**, *36*, 3414.
(32) Livage, J.; Henry, M.; Sanchez, C. *Prog. Solid. State Chem.* **1988**, *18*, 259.
(33) Initial pH values of the reaction mixtures were 0.67, 0.50, and 0.45, and final pH values were 1.37, 1.20, and 1.30, respectively, during the synthesis of AgVPO, CuVPO, and ZnVPO.
(34) Ayyappan, P.; Ramanan, A.; Joy, P. A.; Pring, A. *Solid State Ionics*, in press.